

Supporting Information

Construction of Hierarchical Yolk-Shell Nanospheres Organized by Ultrafine Janus Subunits for Efficient Overall Water Splitting

Qi Zhang, Bingqiu Liu, Yue Ji, Lihua Chen, Lingyu Zhang, Lu Li,* Chungang Wang*

Materials: PAA ($M_w \approx 1800$) was purchased from Sigma-Aldrich (USA). Nickel chloride hexahydrate ($\text{NiCl}_2 \cdot 4\text{H}_2\text{O}$, 98.0%), Isopropyl alcohol (IPA), aqueous ammonia solution ($\text{NH}_3 \cdot \text{H}_2\text{O}$), ammonium molybdate tetrahydrate ($(\text{NH}_4)_6\text{Mo}_7\text{O}_{24} \cdot 4\text{H}_2\text{O}$) and S powders were obtained from Sinopharm Chemical Reagent Beijing Co., Ltd and used without further purification. Deionized water was used in all experiments.

Synthesis of $\text{Ni}(\text{OH})_2/\text{Mo-PAA}$ NSs: In a 250 mL conical flask, a PAA aqueous solution (0.2 g mL^{-1} , 400 μL), $\text{NH}_3 \cdot \text{H}_2\text{O}$ (2 mol L^{-1} , 400 μL) and 150 mg $(\text{NH}_4)_6\text{Mo}_7\text{O}_{24} \cdot 4\text{H}_2\text{O}$ were added in deionized water (50 mL) and ultrasonically dispersed for 30 min. After that, IPA (200 mL) was dripped to the flask under magnetic stirring to form a suspension. Subsequently, 90 mg $\text{NiCl}_2 \cdot 4\text{H}_2\text{O}$ was added into the suspension under magnetic stirring for more than 1 h to obtain the $\text{Ni}(\text{OH})_2/\text{Mo-PAA}$ NSs. The obtained $\text{Ni}(\text{OH})_2/\text{Mo-PAA}$ NSs were centrifuged and dried at 50 °C for 24 h for further experiment.

Synthesis of NiMoO_4 NSs: The highly dispersed Ni-Mo/PAA- NH_4 NSs were annealed from room temperature to 500 °C at a heating rate of 2 °C min^{-1} and then maintained at 500 °C for 3 h in a furnace under the air to obtain the NiMoO_4 NSs.

Synthesis of $\text{NiS}_2/\text{MoS}_2$ NSs: The as-synthesized NiMoO_4 NSs and S powders were put at two independent porcelain-boats with 500 mg S and 50 mg NiMoO_4 at the upstream and downstream side of the furnace, respectively, then the furnace was allowed to anneal at 350 °C for 1 h with a ramp rate of 2 °C min^{-1} under argon atmosphere to obtain the $\text{NiS}_2/\text{MoS}_2$ NSs.

Synthesis of NiS₂ Nanoparticles: The procedure to fabricate NiS₂ nanoparticles are almost the same with NiS₂/MoS₂ NSs, except the addition of (NH₄)₆Mo₇O₂₄·4H₂O.

Synthesis of MoS₂ Nanosheets: 0.3 mmol (NH₄)₆Mo₇O₂₄·4H₂O and 12 mmol CHN₂S were mixed into 70 mL distilled water and stirred for 20 min, then the solution was transferred into a 100 mL Teflon-lined stainless steel autoclave and heated at 180 °C for 12 h to obtain the MoS₂ nanosheets.

Characterization: Transmission electron micrographs (TEM) were taken by JEOLJEM-2100F transmission electron microscope under a 200 kV accelerating voltage. High-resolution TEM (HRTEM) characterizations were recorded by a TECNAI G2 F20 transmission electron microscope under 200 kV accelerating voltage. Scanning electron microscopy (SEM) images were obtained by using an XL30 ESEM-FEG field-emission scanning electron microscope (FEI Co.). X-ray diffraction (XRD) patterns were obtained on a D8 Focus diffractometer with Cu K α radiation. X-ray photoelectron spectroscopy (XPS) was performed with an ECSALAB 250 by using non-monochromated Al K α radiation. N₂ adsorption-desorption measurements were measured using an intelligent gravimetric analyser Autosorb-iQ (Quantachrome).

Electrochemical Tests: 5 mg of the prepared catalysts powder and 10 μ L of Nafion (5 wt %) were added in 1 mL of 4/1(v/v) water/ethanol solution, which was a sonication treatment for 30 min to get homogeneous inks. Then, 5 μ L of the mixed solution was drop-cast onto a glassy carbon electrode (GCE) with a diameter of 3 mm for the electrochemical measurements. All electrochemical experiments were performed in a three-electrode system at room temperature using a CHI760E electrochemical workstation. Catalyst-modified GCE, graphite rod, a saturated calomel electrode (SCE, 0.241V vs. RHE) were used as the working electrode, counter electrode and reference electrode, respectively. LSV curves were measured deaerated with nitrogen with a scan rate of 5 mV s⁻¹ in 1 M KOH aqueous solution at 25 °C prior to the HER and overall water splitting measurements. And the 1 M KOH aqueous

solution was purged with O₂ prior to the OER test. The catalysts were activated using 20 CV scans with a scan rate of 100 mV s⁻¹ before recording the electrochemical performance.

All plots displayed were calibrated to a (RHE) based on the equation ($E_{\text{RHE}} = E_{\text{SCE}} + 0.059 \text{ pH} + 0.241$) and corrected against the iR compensation. EIS was carried out in potentiostatic mode from 0.1 to 10⁵ Hz with AC voltage amplitude of 10 mV. In order to explore the changes in morphology and structure for NiS₂/MoS₂ NSs after the stability test, we fabricated the electrode by loading NiS₂/MoS₂ NSs on commercial carbon cloth (1 cm × 1 cm, mass loading: 3 mg cm⁻²).

The ECSA was calculated through performing the capacitive current associated with double-layer charging from the scan-rate dependence of CVs. The CVs measurements were taken in non-faradic potential window with different scan rate. The C_{dl} of the samples were estimated by plotting the $\Delta J = J_a - J_c$ against the CV scan rate, The linear slope of curves is equivalent to twice of the double-layer capacitance C_{dl}, and the C_{dl} is proportional to the ECSA.

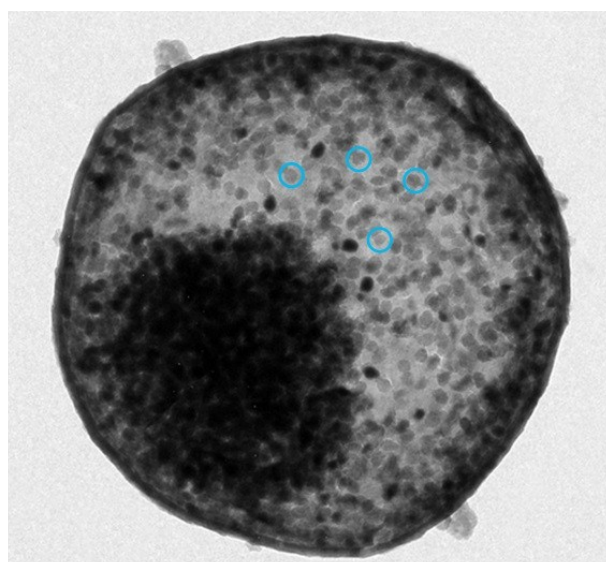


Fig. S1. TEM image of a single NiMoO₄ yolk-shell NS.

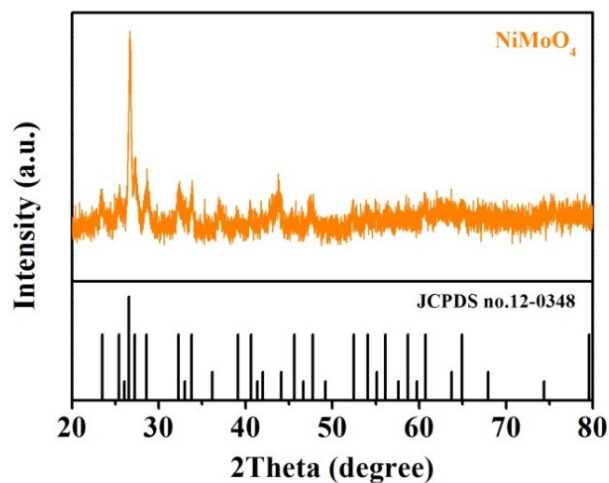


Fig. S2. XRD pattern of the NiMoO₄ yolk-shell NSs.

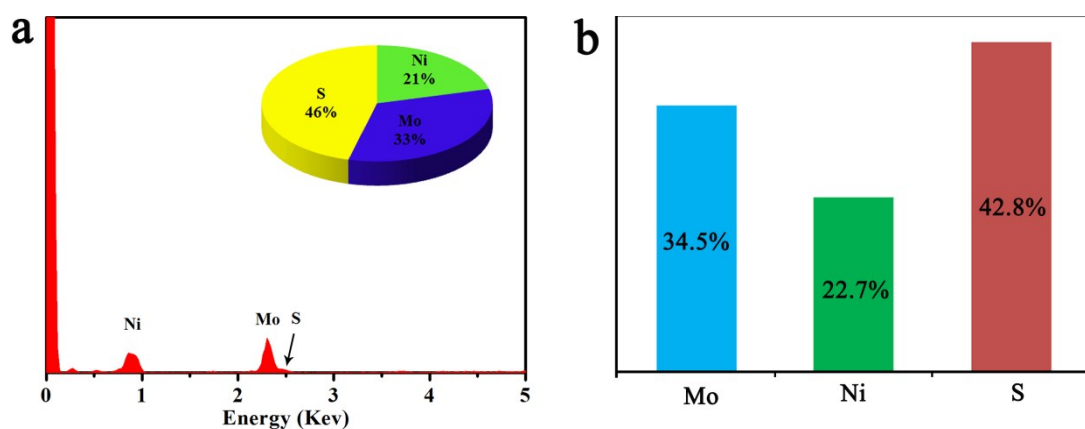


Fig. S3. (a) Energy dispersive X-ray spectrum of NiS₂/MoS₂ yolk-shell NSs. The inset shows the atomic (Ni, Mo and S) contents of NiS₂/MoS₂ yolk-shell NSs. (b) ICP-AES results of NiS₂/MoS₂ yolk-shell NSs.

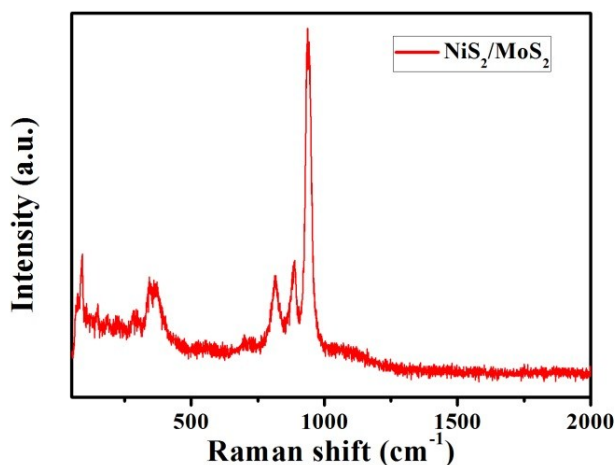


Fig. S4. Raman spectrum of the NiS₂/MoS₂ yolk-shell NSs.

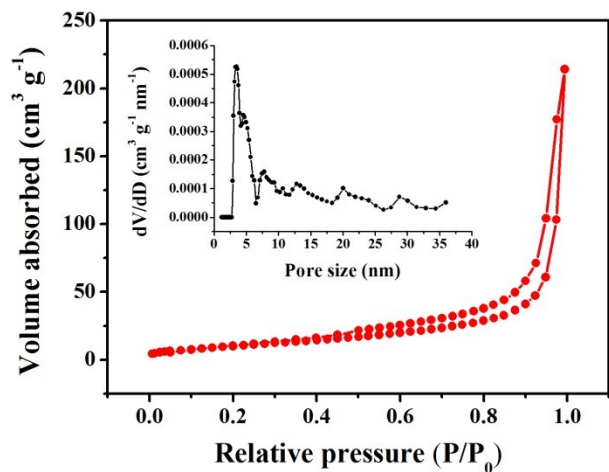


Fig. S5. N₂ adsorption-desorption isotherms and pore size distribution (inset) of NiS₂/MoS₂ yolk-shell NSs.

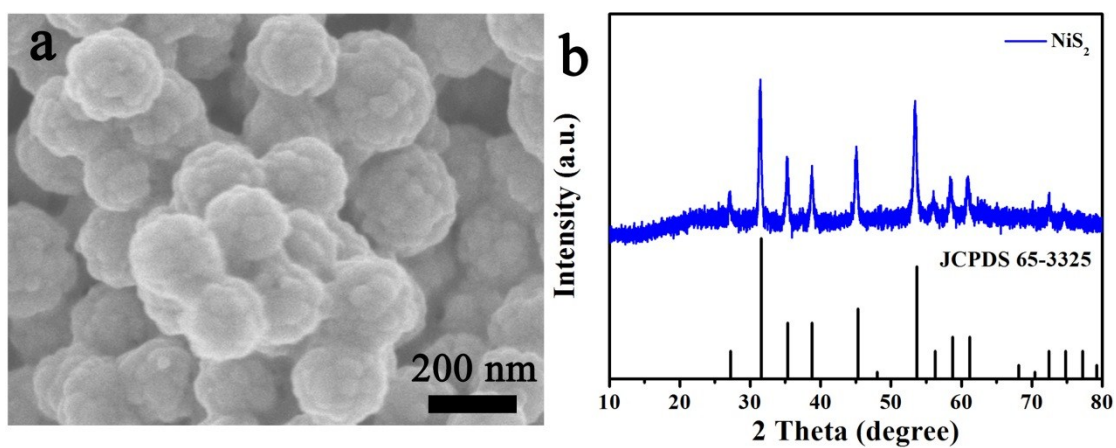


Fig. S6. (a) SEM image, (b) XRD pattern of NiS₂ nanoparticles.

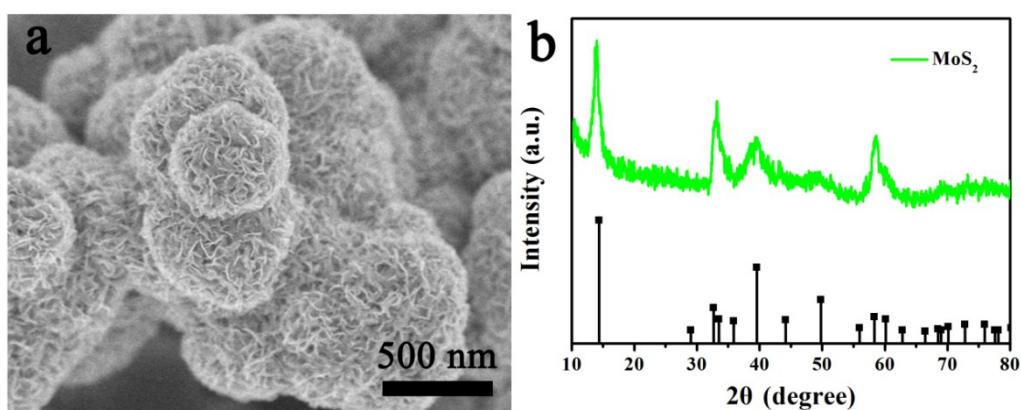


Fig. S7. (a) SEM image, (b) XRD pattern of MoS₂ nanosheets.

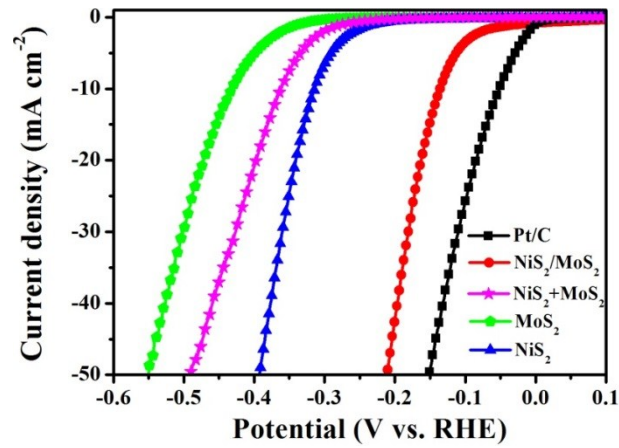


Fig. S8. Polarization curves of NiS₂/MoS₂, NiS₂ + MoS₂, MoS₂, NiS₂ and Pt/C electrodes at a scan rate of 5 mV s⁻¹ for the HER in 1.0 M KOH.

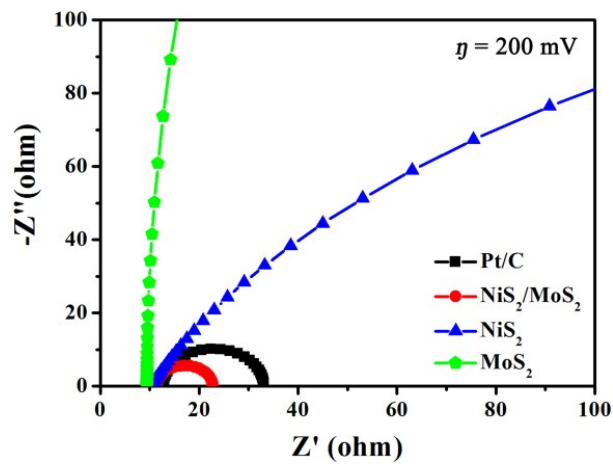


Fig. S9. Nyquist plots of EIS of NiS₂/MoS₂, MoS₂, NiS₂ and Pt/C obtained in 1 M KOH aqueous solutions at an overpotential of 200 mV.

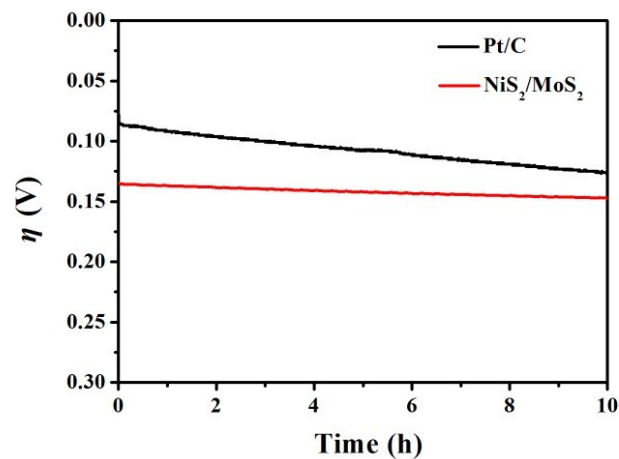


Fig. S10. Time-dependent overpotential of NiS₂/MoS₂ yolk-shell NSs electrode and commercial Pt/C with a constant current density of 10 mA cm⁻² in 1.0 M KOH.

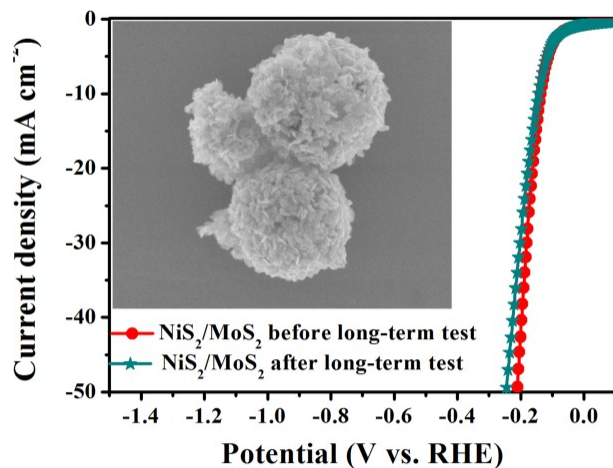


Fig. S11. Polarization curves of NiS₂/MoS₂ yolk-shell NSs before and after long-term HER tests in 1.0 M KOH, inset: the corresponding SEM image after long-term HER tests.

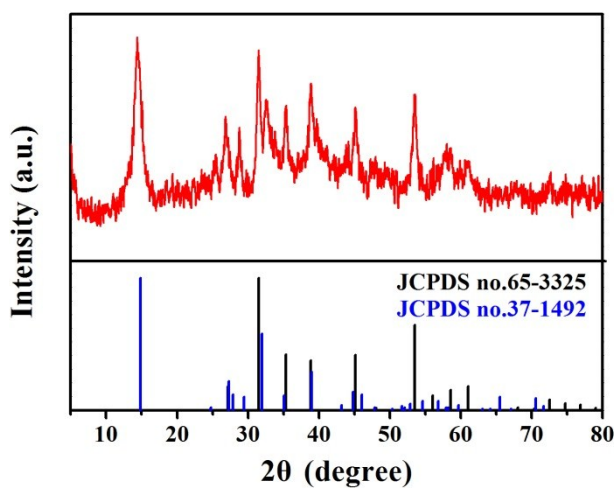


Fig. S12. The XRD pattern of NiS₂/MoS₂ yolk-shell NSs after HER test.

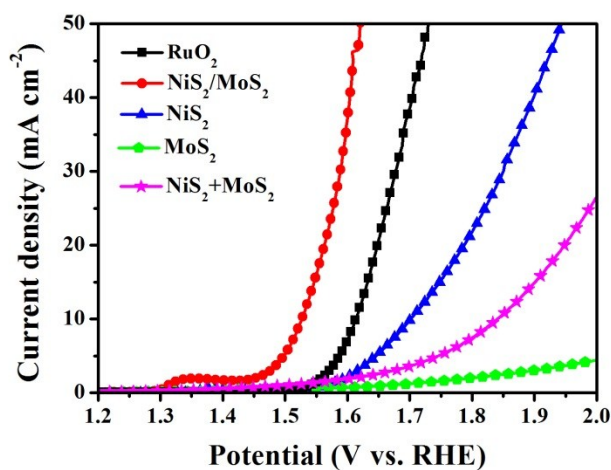


Fig. S13. Polarization curves of NiS₂/MoS₂, NiS₂ + MoS₂, MoS₂, NiS₂ and RuO₂ electrodes at a scan rate of 5 mV s⁻¹ for the OER in 1.0 M KOH.

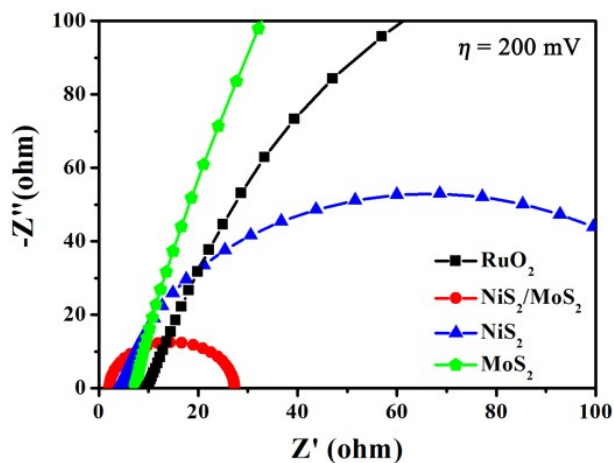


Fig. S14. EIS Nyquist plot of different electrodes recorded at the same applied voltage (1.43 V vs. RHE).

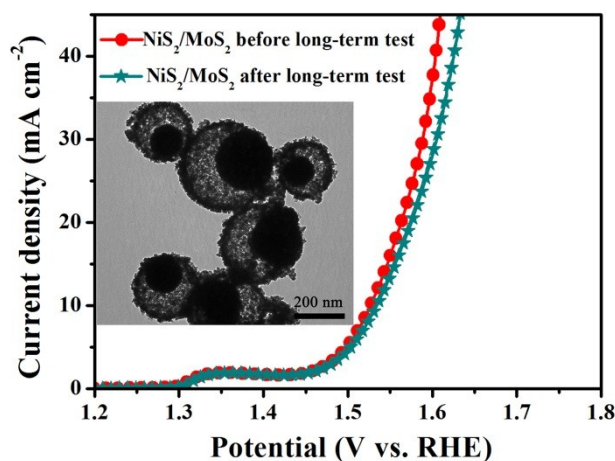


Fig. S15. Polarization curves of NiS₂/MoS₂ yolk-shell NSs before and after long-term OER test in 1.0 M KOH, inset: the corresponding TEM image after long-term HER test.

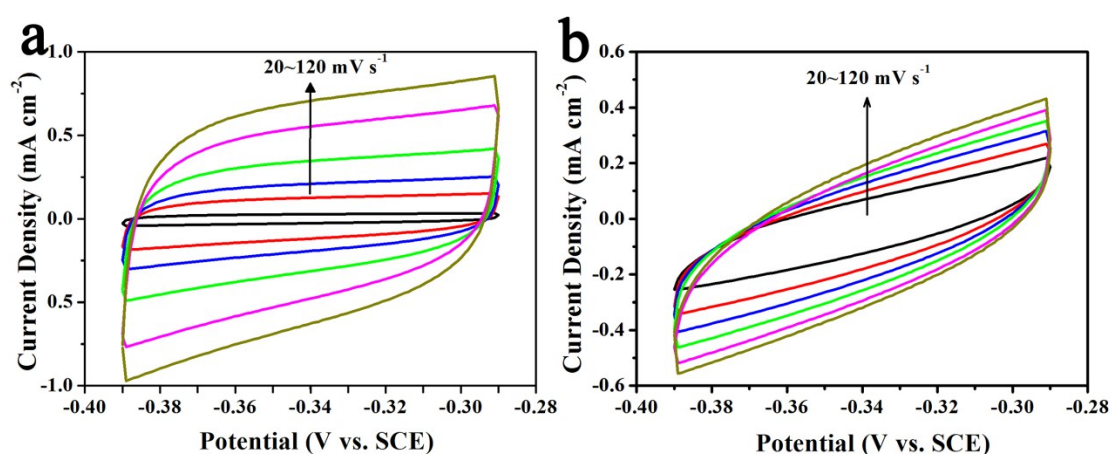


Fig. S16. CVs curves of (a) NiS₂ nanoparticles and (b) MoS₂ nanosheets in 1 M KOH.

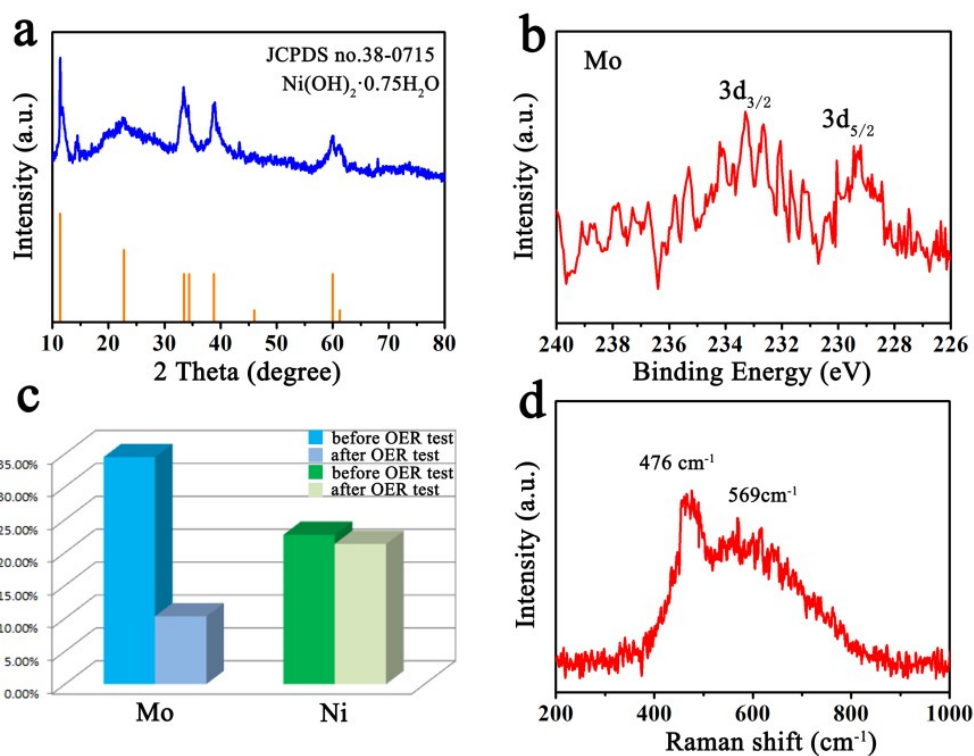


Fig. S17. (a) XRD, (b) XPS spectrum of Mo 3d, (c) ICP-AES results and (d) Raman spectrum of NiS₂/MoS₂ yolk-shell NSs after long-term OER tests.

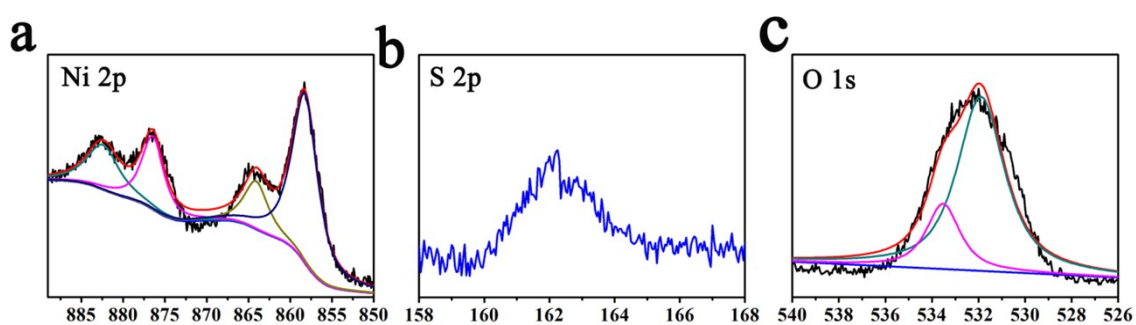


Fig. S18. XPS (a) Ni 2p, (b) S 2p, (c) O 1s spectra of NiS₂/MoS₂ yolk-shell NSs after long-term OER tests.

Table S1. Comparison of the HER performance of NiS₂/MoS₂ yolk-shell NSs with other electrocatalysts

| Catalysts | η_{10} (mV) | Tafel slope (mV·dec ⁻¹) | Electrolyte s | Refs. |
|---|---------------------|--|------------------|--|
| NiS ₂ /MoS ₂ NSs | 135 | 82 | 1 M KOH | this work |
| Ni@NC-800 | 205 | 160 | 1 M KOH | <i>Adv. Mater.</i> 2017 , 29, 1605957 |
| Ni/Ni ₂ P/Mo ₂ C@C | 183 | 66 | 1 M KOH | <i>J. Mater. Chem. A</i> 2018 , 6, 5789 |
| Co phosphide/phosphate | 430 | — | 1 M KOH | <i>Adv. Mater.</i> 2015 , 27, 3175 |
| NiFe LDHNS@DG10 | 300 | 110 | 1 M KOH | <i>Adv. Mater.</i> 2017 , 29, 1700017 |
| Ni _{1.5} Fe _{0.5} P | 282 | 125 | 1 M KOH | <i>Nano Energy</i> 2017 , 34, 472 |
| Ni ₁₂ P ₅ | 270 | — | 1 M KOH | <i>ACS Catal.</i> 2017 , 7, 103 |
| c-CoSe ₂ /CC | 190 | 85 | 1 M KOH | <i>Adv. Mater.</i> 2016 , 28, 7527 |
| NiMo ₃ S ₄ | 252 | 98 | 0.1 M KOH | <i>Angew. Chem. Int. Ed.</i> 2016 , 55, 1–6 |
| ONPPGC/ OCC | 446 | 154 | 1 M KOH | <i>Energy Environ. Sci.</i> 2016 , 9, 1210–1214 |
| Ni _{1-x} Fe _x /NC | 230 | 111 | 1 M KOH | <i>ACS Catal.</i> 2016 , 6, 580–588 |
| NiCo ₂ S ₄ @NiFe LDH/NF | 200 | 101 | 1 M KOH | <i>ACS Appl. Mater.</i> <i>Interfaces.</i> 2017 , 9 15364 |
| Co-NRCNTs | 370 | — | 1 M KOH | <i>Angew. Chem. Int. Ed.</i> |

Table S2. Comparison of the OER performance of NiS₂/MoS₂ NSs with other electrocatalysts

| Catalysts | η_{10} (mV) | Tafel slope (mV·dec⁻¹) | Electrolyte s | Refs. |
|--|--|--|--------------------------|---|
| NiS ₂ /MoS ₂ NSs | 293 | 102.3 | 1 M KOH | this work |
| Ni/Mo ₂ C-PC | 368 | — | 1 M KOH | <i>Chem. Sci.</i> 2017 , 8, 968 |
| NiCo LDH | 367 | 183 | 1 M KOH | <i>Nano Lett.</i> 2015 , 15, 1421 |
| Co ₃ O ₄ /NiCo ₂ O ₄ | 340 | 88 | 1 M KOH | <i>J. Am. Chem. Soc.</i> 2015 , 137, 5590 |
| NiFe LDHNS@DG10 | 300 | 110 | 1 M KOH | <i>Adv. Mater.</i> 2017 , 29, 1700017 |
| CoO/NG | 340 | 71 | 1 M KOH | <i>Energy Environ. Sci.</i> 2014 , 7, 609 |
| NiCo(OH) _x | 410 | 109 | 1 M KOH | <i>Adv. Energy Mater.</i> 2015 , 5, 1401880 |
| c-CoSe ₂ /CC | 190 | 85 | 1 M KOH | <i>Adv. Mater.</i> 2016 , 28, 7527 |
| NiMoP ₂ | 330 | 90.6 | 1 M KOH | <i>J. Mater. Chem. A</i> 2017 , 5, 7191 |